Heliyon 10 (2024) e30518

Contents lists available at ScienceDirect

Heliyon

journal homepage: www.cell.com/heliyon

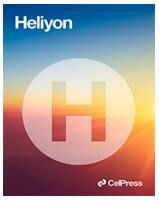

Research article

Cytotoxicity of amine-modified polystyrene MPs and NPs on neural stem cells cultured from mouse subventricular zone

Ki-Youb Park [a,*], Man Su Kim [b], Nuri Oh [a]

[a] Department of Chemistry and Biology, Korea Science Academy of KAIST, 105-47 Baegyanggwanmun-ro, Busanjin-Gu, Busan, 47162, South Korea
[b] College of Pharmacy, Inje University, Gimhae, 50834, South Korea

ARTICLE INFO

Keywords:
Microplastics
Nanoplastics
Polystyrene
Subventricular zone
Neural stem cell
Cytotoxicity

ABSTRACT

Microplastics (MPs) and nanoplastics (NPs) are found in various environments such as aquatic, terrestrial, and aerial areas. Once ingested and inhaled, these tiny plastic debris damaged the digestive and respiratory organ systems in animals. In humans, the possible connection between MPs and various diseases such as lung diseases has been raised. Yet, the impact of MPs on the human nervous system has been unclear. Previous research using animals and cultured cells showed possible neurotoxicity of MPs and NPs. In this study, we used neural stem cells cultured from mouse subventricular zone to examine the effects of polystyrene (PS) NPs and MPs with sizes of 0.1 μm, 1 μm, and 2 μm on the cell proliferation and differentiation. We observed that only positively charged NPs and MPs, but not negatively charged ones, decreased cell viability and proliferation. These amine-modified NPs and MPs decreased both neurogenesis and oligodendrogenesis. Finally, fully differentiated neurons and oligodendrocytes were damaged and removed by the application of NPs and MPs. All these effects varied among different sizes of NPs and MPs, with the greatest effects from 1 μm and the least effects from 2 μm. These results clearly demonstrate the cytotoxicity and neurotoxicity of PS-NPs and MPs.

1. Introduction

MPs are plastic particles with a diameter less than 5 mm. They can be intentionally made for products like abrasive cleaners or byproducts of deteriorating plastic materials such as plastic bottles, clothes, and cosmetics [1]. With a high use of plastic products with an estimate of at least 381 million tons in 2018 year alone, the degraded debris, MPs, represent growing sources of pollution in aquatic environments [2] and terrestrial environments [3]. Airborne MPs have been detected in human lung tissue, indicating possible inhalation of MPs [4]. Meta-analysis of publications suggested that humans may ingest 0.1–5 g of MPs weekly [5]. The potential negative impacts of MPs on human health have been much reported. Upon ingestion, MPs possibly damage the intestinal barrier function in human gut [6]. Their possible contributions to human cardiovascular diseases [7], carcinogenesis [8], and lung diseases [9] have been raised. Yet, further research on the impacts of MPs on human health is required.

Since its first production in 1930s, PS has been widely used as a solid material or used to make Styrofoam, which can be used to produce food containers, office supplies, and more [10]. Toxic effects of PS-MPs and -NPs on aquatic species, mammals, and human cells have been reported [11]. Adult zebrafish exposed to PS-MPs experienced hepatic glycolipid metabolism disorder [12]. In black rockfish *Sebastes schlegelii*, PS-MPs caused incapable hunting behavior along with signs of respiratory stress [13]. Rats exposed to

* Corresponding author.
E-mail address: kiyoubpark@ksa.kaist.ac.kr (K.-Y. Park).

https://doi.org/10.1016/j.heliyon.2024.e30518
Received 1 April 2024; Received in revised form 27 April 2024; Accepted 29 April 2024
Available online 7 May 2024

PS-MPs showed cardiovascular toxicity [14]. Mice exposed to PS-MPs experienced damage in hepatic lipid metabolism [15]. PS-MPs exerted cytotoxicity in cultured human kidney proximal tubular epithelial cells HK-2 by damaging mitochondria and endoplasmic reticulum [16]. Additionally, PS-MPs induced reactive oxygen species and decreased transepithelial electrical resistance in human lung epithelial BEAS-2B culture cells [17]. Therefore, PS-MPs seem to have toxic effects on various organs in many species along the food chain.

Neurotoxicity of PS-MPs and -NPs in rodents and neural culture cells has been reported. Exposure to PS-MPs impaired learning and memory in mice [18]. PS-NPs with a size of 50 nm were shown to pass through the blood-brain barrier and cause microglial activation in mice [19]. Chronic exposure to PS-MPs decreased social novelty preferences in mice, suggesting possible neurotoxicity [20]. Long-term exposure to PS-MPs reduced cell viability in human forebrain cortical spheroids [21] and increased anxiety-like behaviors in adult mice [22]. Ingestion of PS-NPs caused neuronal degeneration in the hippocampi of rats [23]. All these reports suggest that PS-MPs and PS-NPs can penetrate the mammalian brain and exert neurotoxicity.

The subventricular zone (SVZ) is the brain region with neural stem cells (NSCs) that can generate neurons and glial cells throughout the lifetime [24]. NSCs cultured from the SVZ can be differentiated to neurons, oligodendrocytes, and astrocytes by replacing the growth medium with differentiating medium that lacks growth factors and serum [25]. Therefore, SVZ NSCs are a good model system for researching the effects of chemical and biological reagents on the neuronal and glial cell differentiation [26,27]. In this study, we treated NSCs cultured from the mouse SVZ with various sizes of PS-MPs and -NPs. We observed that PS-MPs and PS-NPs of 0.1 μm, 1 μm, 2 μm sizes reduced cell viability and mitotic cell division, which was dependent on the dose and surface charge of MPs and NPs. Only positively charged amine-modified MPs and NPs reduced cell viability. PS-MPs and -NPs inhibited neuronal differentiation and oligodendrogenesis. PS-MPs and -NPs were cytotoxic to differentiated neurons and oligodendrocytes. To our knowledge, this is the first detailed study about the effects of PS-MPs and -NPs on SVZ NSCs.

2. Materials and methods

2.1. Characterization of polystyrene microplastic and nanoplastic beads

In this study, all PS-MPs and -NPs were latex beads with a fluorescence tag and purchased from Sigma Aldrich. The list of polystyrene beads is shown in Table 1. All of them were in aqueous suspension with a 2.5 % stock concentration. To apply to cells, the stock solution was diluted in the culture medium.

To measure the hydrodynamic size (HD) and zeta potential (ZP), PS NPs and MPs were diluted in distilled water at a 1:100 dilution. HD and ZP were measured at 25 °C using a dynamic light scattering (DLS) instrument (Malvern Instruments, Malvern, UK).

2.2. NSC culture

NSCs were obtained from SVZ tissue from 5-day-old mouse pups of the CD1 mouse strain (Orient Bio, Korea) after euthanization using carbon dioxide. The euthanization process was performed following the protocol approved by Inje University Animal Care and Use Committee (approval ID number: Inje 2020-006). The process of obtaining SVZ tissue and NSC culture conditions was previously reported [27]. In short, the brain slice was cut in a way to contain the lateral ventricles. The lower part of the lateral ventricles was cut and dissociated using trypin (Gibco, ThermoFisher, Waltham, MA, USA). Cells were plated at a density of SVZ tissues from one pup into one well of 6-well culture plate. These cells were passage 0 (P0) and incubated for one week. Then, cells were passaged at a 1:2 or 1:3 split ratio every two or three days. In this study, passage 4 to 7 cells were used for experiments. Cells were incubated at 37 °C with 5 % carbon dioxide. The growth medium (N5) consists of DMEM/F12-GlutaMAX™ supplemented with 5 % fetal bovine serum (GenDEPOT, Texas, USA), 10 % N2 supplement, 35 μg/mL bovine pituitary extract, 20 ng/mL epidermal growth factor (EGF), 20 ng/mL basic fibroblast growth factor (bFGF), and 10 % antibiotic/antimycotic. All materials in the culture medium were from Gibco (ThermoFisher, Waltham, MA, USA), except for fetal bovine serum.

2.3. Cell viability assay

The NSCs were plated into a 96-well plate. The next day, the culture medium was switched with 100 μl of new culture medium containing PS-MPs and -NPs beads per well. After one day of incubation, 10 μl of Quanti-Max™ WST-8 reagent (BIOMAX, Seoul, Korea) was added to each well and incubated for 1 h at 37 °C with 5 % carbon dioxide. Cell viability was measured by optical density at 450

Table 1
Fluorescent tagged PS-MPs and PS-NPs used in this study.

Polystyrene NPs, MPs	Surface modification	Surface charge	Fluorescence Excitation	Fluorescence Emission
0.1 μm	Sulfate	–	~520 nm	~540 nm
0.1 μm	Amine	+	~475 nm	~540 nm
1 μm	Carboxylate	–	~470 nm	~505 nm
1 μm	Amine	+	~470 nm	~505 nm
2 μm	Carboxylate	–	~470 nm	~505 nm
2 μm	Amine	+	~520 nm	~540 nm

nm light (OD450) with a VersaMax microplate reader (Molecular Devices, San Jose, CA, USA). Medium without cells was used as a blank measurement, and all OD450 values were normalized with the blank measurement.

2.4. 5-ethynyl-2′-deoxyuridine (EdU) assay

The NSCs were plated at a 1:4 split ratio on 8-well CC2 chamberslides (Nunc, ThermoFisher, Waltham, MA, USA) coated with laminin (Invitrogen, ThermoFisher, Waltham, MA, USA) overnight. The next day, the medium was replaced with fresh medium containing 10 μg/ml PS-MPs or NPs, and cells were incubated for 18 h. For EdU incorporation, cells were incubated in N5 medium containing 5 μM EdU for 1 h. The EdU detection assay was performed following manufacturer's protocol of the Click-iT Plus EdU Imaging Kit (Invitrogen, ThermoFisher, Waltham, MA, USA). Briefly, cells were fixed in 4 % paraformaldehyde for 15 min and then, permeabilized with 0.5 % Triton X-100 for 20 min. Cells were incubated in EdU detection cocktail for 30 min, followed by 4′,6-diamidino-2-phenylindole (DAPI) staining (1:1000 diluted in phosphate buffered saline (PBS)) for 30 min. Between different solutions, 3 % bovine serum albumin (Sigma, St. Louis, MO, USA) in PBS was used for washing. After imaging with the fluorescence microscope (Olympus, Tokyo, Japan), EdU-positive cells and DAPI-stained cells were counted using a cell count macro in iSolution software (IMT i-Solution Inc., Vancouver, BC, Canada).

2.5. Lactate dehydrogenase (LDH) assay

The NSCs (12×10^3 cells per well) were plated on 96-well plate coated with laminin/poly-D-lysine coating solution (Sigma, St. Louis, MO, USA). Next day, the cells were briefly rinsed with differentiation medium (N6) and incubated in fresh N6 medium containing 10 μg/ml PS-MPs or NPs. N6 medium is the same as the growth N5 medium except for the lack of EGF, bFGF, and fetal bovine serum. After 18-hr incubation, LDH cytotoxicity assay was performed using Quanti-LDH™ PLUS cytotoxicity assay kit, following the manufacturer's instructions (BIOMAX, Seoul, Korea). The absorbance at 490 nm was measured using a VersaMax microplate reader (Molecular Devices, San Jose, CA, USA). N6 Medium without cells was used as a blank measurement, and all OD490 values were normalized with the blank measurement.

2.6. Lysotracker labeling

The NSCs were plated on laminin (Invitrogen, ThermoFisher, Waltham, MA, USA) -coated 8-well CC2 chamberslides (Nunc, ThermoFisher, Waltham, MA, USA). The next day, cells were treated with N5 medium containing 5 μg/ml 0.1 μm amine-modified PS beads for 12 h. Then, cells were incubated in fresh N5 medium containing 100 nM LysoTracker and 1X Hoechest 33342 (diluted in Live Cell Imaging Solution) for 5 min in the 37 °C incubator. After rinsing three times with fresh Live Cell Imaging Solution, the cells were imaged. All reagents are from Molecular Probes (ThermoFisher, Waltham, MA, USA).

2.7. Differentiation of NSCs

NSCs were plated onto laminin coated 8-well CC2 chamberslides at a 1:1 or 1:2 split density. After one day, the culture medium is briefly rinsed with N6 medium, and then the cells were treated with fresh N6 or N6 medium containing PS-MPs and -NPs beads. For transient exposure with PS-MPs and -NPs beads, medium containing PS beads was removed and then, cells were rinsed with fresh N6 medium 3 times. Then, fresh N6 medium was added to the cells. For long-term differentiation, fresh N6 medium was added at 4 days of differentiation. At 8 days of differentiation, N6 medium containing PS beads was added to the cells.

2.8. Immunocytochemistry and fluorescence imaging

Similar procedures as previously described [27] were performed for immunocytochemistry. Cells were rinsed with PBS briefly and then fixed in 4 % paraformaldehyde (Sigma, St. Louis, MO, USA) for 15 min or 30 min. After 30 min of blocking with 10 % normal goat serum (Cell Signaling, Danvers, MA, USA) with 0.1–0.3 % Triton X-100 (Sigma, St. Louis, MO, USA), cells were incubated in the blocking solution containing primary antibodies for 2 h. After briefly rinsing with PBS, cells were incubated in PBS containing secondary antibodies and DAPI (Sigma, St. Louis, MO, USA) for 30 min. Cells were mounted using Aqua-Poly/Mount (Polysciences, Warrington, PA, USA). The primary antibodies were mouse anti-Tuj1 (BioLegend, San Diego, CA, USA), rabbit anti-Olig2, and rabbit anti-histone H3 phosphorylated at Ser10 (PH3). Both Olig2 and PH3 antibodies were purchased from Millipore, Billerica, MA, USA. The secondary antibodies were Alexa-488-conjugated anti-mouse and Alexa-594-conjugated anti-rabbit. Secondary antibodies were from Jackson ImmunoResearch, West Grove, PA, USA. All primary and secondary antibodies were diluted at 1:500.

For fluorescence imaging, three or four wells of cells per condition were imaged using a fluorescence microscope (Olympus, Tokyo, Japan). For cell counting, 5 fields of view per well were randomly imaged. The number of Tuj1-positive cells was counted manually. The numbers of Olig2-positive cells and DAPI-positive cells were automatically counted using a cell count macro in iSolution software (IMT i-Solution Inc., Vancouver, BC, Canada).

2.9. Statistical analysis

All the quantified datasets were analyzed with one-way ANOVA analysis and F statistic value was greater than F critical value in all

of the analysis, indicating the presence of differences among groups. Then, post-hoc analysis using the Bonferroni correction was performed along with Student's *t*-test (two-tailed distribution and two-sample equal variance). When the *p*-value was less than 0.05 or 0.01, statistical significance was indicated in the graphs. The number of biologically independent experiments is indicated as N (for example, N = 3) in the relevant figure legends.

A

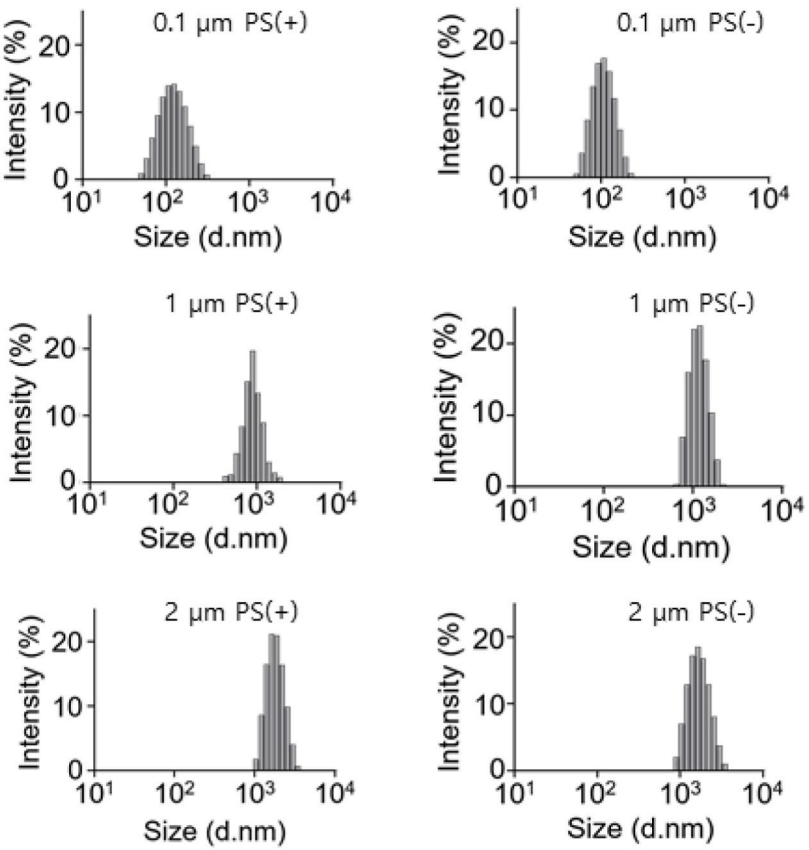

B

Polystyrene NPs, MPs	Surface modification	HD [d.nm]	ZP [mV]
0.1 μm PS(+)	Amine	140.17 ± 2.43	69.5 ± 1.16
0.1 μm PS(-)	Sulfate	108.12 ± 1.65	-20.5 ± 0.89
1 μm PS(+)	Amine	981.08 ± 1.29	58.2 ± 2.80
1 μm PS(-)	Carboxyl	1385.02 ± 1.92	-56.3 ± 3.21
2 μm PS(+)	Amine	1952.45 ± 1.15	10.4 ± 1.22
2 μm PS(-)	Carboxyl	1748.03 ± 2.88	-28.8 ± 1.72

Fig. 1. (A) Representative histograms of hydrodynamic (HD) size distribution of polystyrene NPs and MPs of 0.1, 1, and 2 μm in diameter (d. nm) with positive (+) or negative (−) surface charge. (B) The surface modification, HD, and zeta potential (ZP) of each polystyrene beads. All data are means ± S.D. (n = 3).

3. Results

3.1. Characterization of polystyrene microplastic and nanoplastic beads

The sizes and zeta potentials of PS-MPs and -NPs were measured using dynamic light scattering (DLS). The hydrodynamic (HD) size distribution indicated that the peak intensity was at the expected size 0.1, 1, and 2 μm (Fig. 1A). The mean sizes (HD) of 0.1 μm amine-modified PS, 0.1 μm sulfate-modified PS, 1 μm amine-modified PS, 1 μm carboxyl-modified PS, 2 μm amine-modified PS, and 2 μm carboxyl-modified PS were 140.17, 108.12, 981.08, 1385.02, 1952.45, and 1748.03 nm, respectively (Fig. 1B). Additionally, zeta potential (ZP) values reflected the surface charges resulting from chemical modifications, amine-, carboxyl-, or sulfate-coating (Fig. 1B).

3.2. Decreased cell viability by polystyrene microplastic and nanoplastic beads

To investigate the cellular toxicity of PS-MPs and -NPs on cultured NSCs, PS beads with different sizes and charges were applied to proliferating NSCs. Amine-modified PS-MPs and -NPs with sizes of 0.1 μm, 1 μm, and 2 μm were added at concentrations of 20 μg/ml, 40 μg/ml, and 100 μg/ml to the growth medium for 1 day. Compared to the no-beads control group, cells treated with beads showed decreased cell viability. The 0.1 μm-sized PS beads reduced cell viability to one-quarter at concentrations of 20, 40, and 100 μg/ml (Fig. 2A). The 1 μm-sized PS beads decreased cell viability in a dose-dependent manner, reducing it to one-half at 20 μg/ml, one-quarter at 40 μg/ml, and one-eighth at 100 μg/ml compared to the control (Fig. 2A). The 2 μm-sized PS beads reduced cell viability to one-half at concentrations of 20, 40, and 100 μg/ml (Fig. 2B). To compare the effects of surface charge, sulfate- or carboxylate-modified PS beads of the same size were added. None of the negatively charged PS beads significantly decreased the cell viability, while positively charged amine-modified PS beads consistently decreased it (Fig. 2C). Therefore, amine-modified PS beads

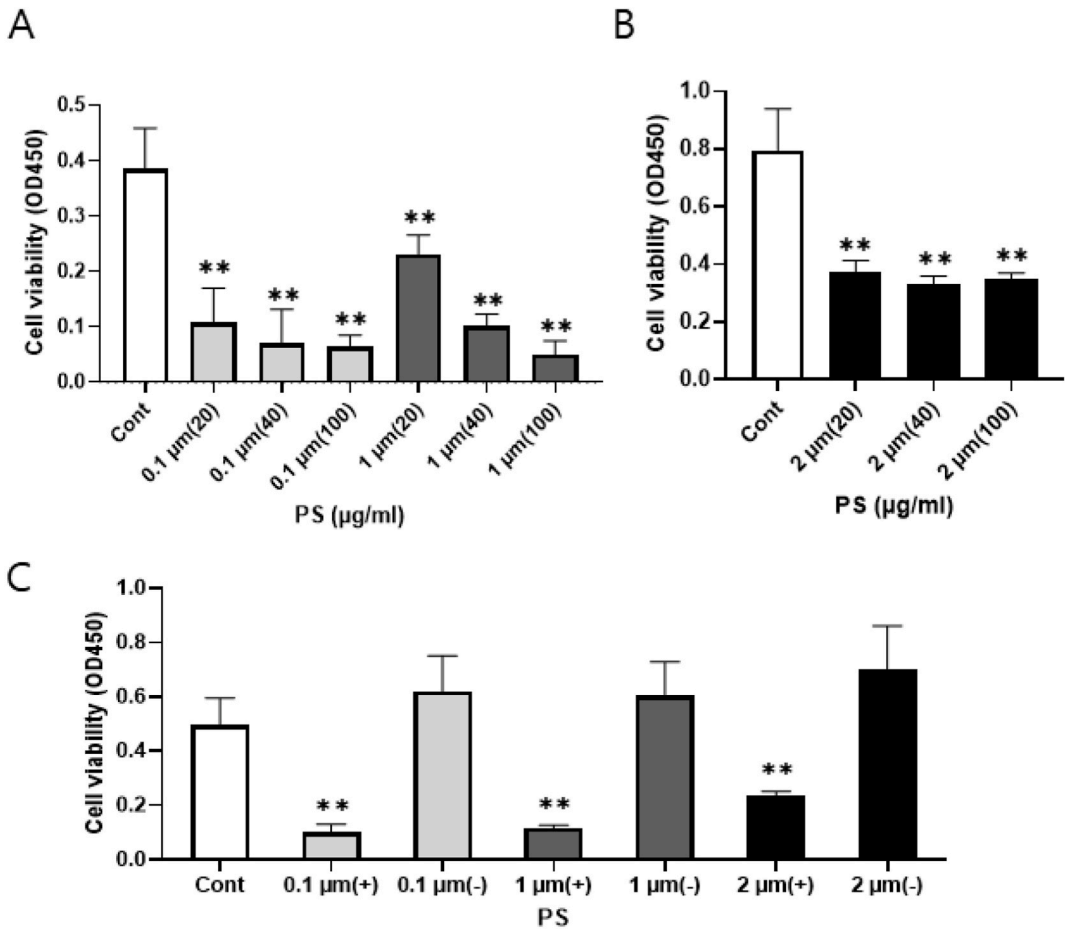

Fig. 2. Reduced cell viability of cultured SVZ NSCs by (A) 0.1 μm, 1 μm, and (B) 2 μm polystyrene beads (PS) at 20, 40, and 100 μg/ml concentrations. (C) Effects of the surface charge (+ or -) of each PS-MPs and -NPs at 40 μg/ml on the cell viability of cultured SVZ NSCs. (A)~(C) Mean and S.E. are shown (N = 3). Statistical analysis was done using one-way ANOVA and Bonferroni correction for pair-wise comparison to no beads control (Cont) (**$p < 0.01$).

were used for the following experiments.

The decrease in cell viability might be attributed to a reduction in cell proliferation. To investigate this possibility, cells were immunostained for a mitotic marker, phosphorylated histone H3 (PH3), after incubation with PS beads. All sizes of PS beads (0.1 μm, 1 μm, or 2 μm) at a concentration of 10 μg/ml significantly decreased the number of PH3-positive cells (Fig. 3A). While 3.6 % of control NSCs were positive for PH3, only 2.0 %, 1.5 %, and 2.1 % of NSCs exposed to 0.1 μm, 1 μm, or 2 μm PS beads, respectively, showed positivity for PH3 (Fig. 3B). Additionally, an EdU assay, which detects cells actively synthesizing DNA during the S phase, was performed (Fig. 3C). While 27 % of control NSCs incorporated EdU into their nuclei, 12 %, 5 %, and 14 % of NSCs exposed to 10 μg/ml of 0.1 μm, 1 μm, or 2 μm PS beads, respectively, exhibited EdU incorporation into their nuclei (Fig. 3D). These results suggest that PS beads decrease cell viability by inhibiting cell division.

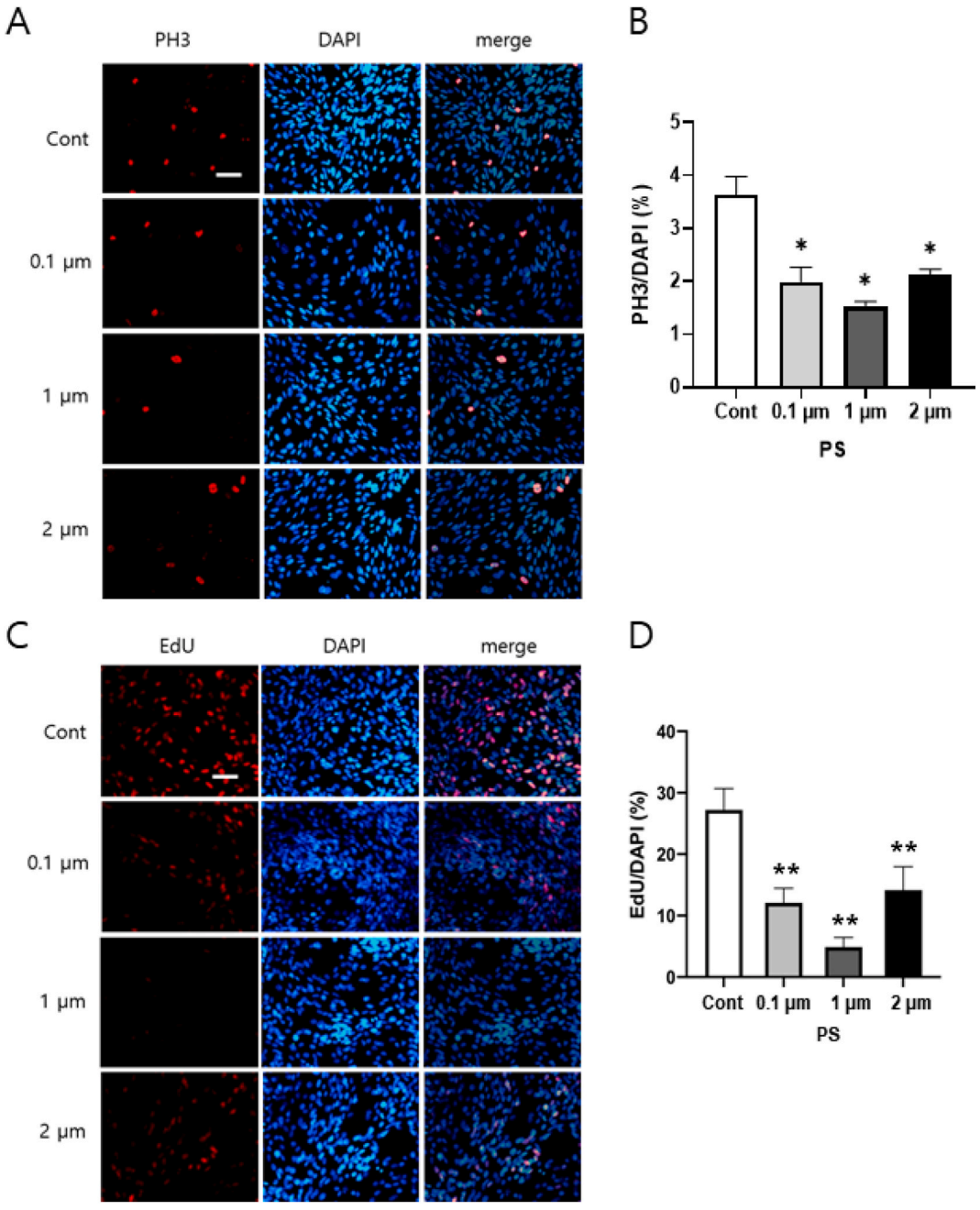

Fig. 3. Decreased PH3-positive cells (A and B) and EdU-positive cells (C and D) in SVZ NSCs cultured with 10 μg/ml PS-MPs and –NPs. The means and S.D. (in (B), N = 1) or S.E. (in (D), N = 3) are shown. Statistical analysis was done using one-way ANOVA and Bonferroni correction for pairwise comparison to no beads control (*$p < 0.05$) in (B) and (**$p < 0.01$) in (D). Scale bar in (A) and (C) is 50 μm.

3.3. Cellular localization of 0.1 μm PS beads

Green fluorescence from 0.1 μm PS beads was observed inside the cells, while 1 μm and 2 μm PS beads appeared to be located outside the cells (data not shown). Therefore, the subcellular localization of 0.1 μm PS beads was examined using fluorescence microscopy in conjunction with the Lysotracker reagent, which accumulates in acidic vesicles within the cell. Co-localization of 0.1 μm PS beads with some Lysotracker labeling (Fg. 4) suggests that the endocytosed 0.1 μm PS beads may have been transported to the lysosomes of proliferating NSCs.

3.4. Inhibition of neurogenesis and oligodendrogenesis by microplastic beads

The effects of PS microplastic beads on differentiation of NSCs were investigated. NSCs were incubated in differentiation medium supplemented with PS beads of sizes 0.1, 1, and 2 μm at concentrations of 1 or 5 μg/ml for 4 days. Immunostaining for the neuronal marker Tuj1 and oligodendrocyte marker Olig2 was performed. At 1 μg/ml, PS beads of all sizes did not significantly affect the neurogenesis and oligodendrogenesis (data not shown), but at 5 μg/ml, they decreased both (Fig. 5A). Specifically, at 5 μg/ml, 0.1 μm and 1 μm PS beads greatly reduced the number of Tuj1-positive cells and Olig2-positive cells (Fig. 5B). Addition of 2 μm PS beads to differentiating cells did not significantly alter the number of Tuj1-positive cells but halved the number of Olig2-positive cells compared to the no-beads control (Fig. 5B). To investigate the potential cause of reduced differentiation, a lactate dehydrogenase (LDH) activity assay was conducted. LDH is released from cells and undergoes enzymatic reaction outside the cell when the plasma membrane is damaged. Compared to the no-beads control NSCs, 1 μm PS beads significantly increased LDH cytotoxicity by 2.8-fold, while 0.1 and 2 μm PS beads showed a slight increase in LDH cytotoxicity, although not statistically significant (Fig. 5C).

Instead of exposing NSCs to PS beads throughout the entire differentiation process, a transient exposure approach was adopted. Specifically, PS beads were added to the cells during the initial two days of differentiation. NSCs were treated with PS beads at a concentration of 10 μg/ml for the first two days of differentiation, followed by continued differentiation for an additional two days in the absence of PS beads (Fig. 6A). Consistent with the findings in Fig. 4, both 0.1 μm and 1 μm PS beads greatly inhibited neurogenesis, whereas 2 μm PS beads did not significantly affect the number of Tuj1-positive neurons (Fig. 6B and C, left). However, oligodendrogenesis was greatly suppressed by all sizes of PS beads (Fig. 6B and C, right), aligning with the observations in Fig. 5. Thus, it appears that transient exposure to 0.1 μm or 1 μm PS beads, particularly during the early stages of differentiation, inhibits both neurogenesis and oligodendrogenesis.

3.5. Cytotoxic effects of PS microplastic beads on neurons and oligodendrocytes

Subsequently, the impact of PS beads on the differentiated neurons and oligodendrocytes derived from NSCs was investigated. NSCs underwent differentiation for 8 days, after which 5 μg/ml PS beads were introduced into the differentiation medium. Following 3 days of incubation in the presence of PS beads, cells were subjected to immunocytochemistry (Fig. 7A). Specifically, 1 μm PS beads led to a reduction in the number of Tuj1-positive cells and Olig2-positive cells, whereas other PS beads (0.1 μm and 2 μm) did not yield significant effects (Fig. 7B). Upon extending the incubation period in the presence of PS beads to 5 days (Fig. 7C), all PS beads with sizes of 0.1, 1, or 2 μm decreased the number of Tuj1-positive neurons (Fig. 7D, left). Regarding oligodendrocytes, only 1 μm PS beads reduced the number of Olig2-positive cells, while 0.1 μm and 2 μm beads did not elicit significant effects (Fig. 7D, right). These findings suggest that PS beads (0.1, 1, and 2 μm) may induce neurotoxicity upon prolonged exposure of neurons to PS-MPs or –NPs.

4. Discussion

In this research, we investigated the effects of PS-MPs and -NPs with different sizes. All sizes of MPs and NPs (0.1, 1, and 2 μm) exhibited a similar decrease in cell viability in cultured NSCs. Among them, 1 μm MP showed the most pronounced effect in reducing cell proliferation, as indicated by PH3 immunostaining and EdU incorporation assays. Furthermore, 1 μm MP nearly completely inhibited neurogenesis of NSCs when applied for four days or during the initial two days of differentiation. When added to NSC-derived cells undergoing differentiation for 8 days, 1 μm MP resulted in a notable absence of neurons and a significant reduction in the number of Olig2-positive oligodendrocytes. These effects may be attributed to damaged plasma membrane integrity, as evidenced by increased LDH cytotoxicity. NPs with a size of 0.1 μm exhibited similar effects to 1 μm MP but to a lesser extent. Conversely, 2 μm MP did not

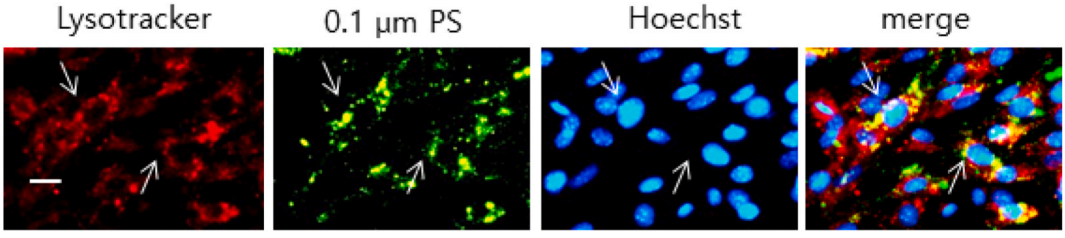

Fig. 4. Co-localization of 0.1 μm PS beads with Lysotracker as indicated with arrows. Scale bar is 10 μm.

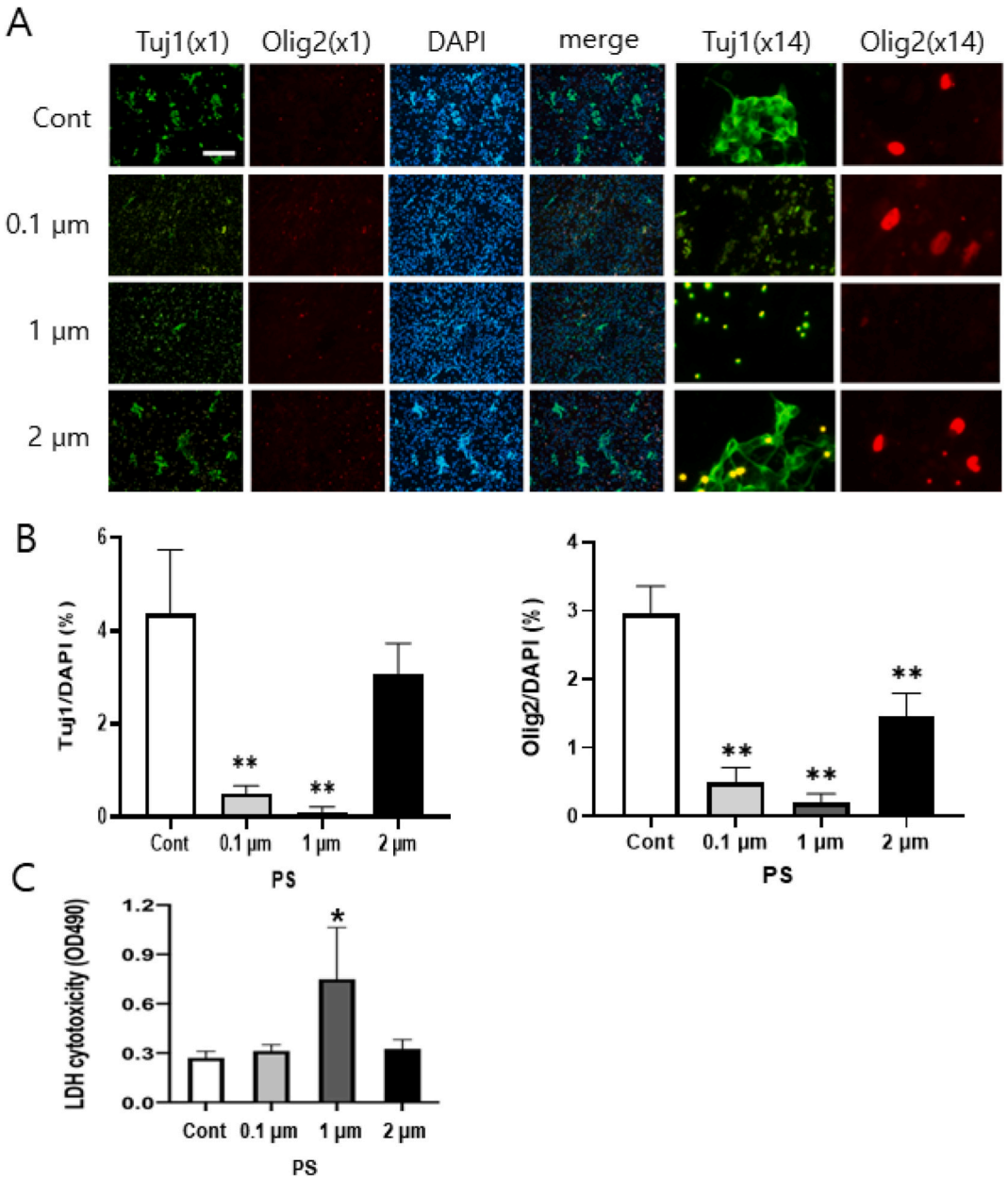

Fig. 5. (A) PS-MPs and -NPs inhibited differentiation of SVZ NSCs to neurons (Tuj1) and oligodendrocytes (Olig2) after 4-day differentiation in the presence of 5 μg/ml PS beads. Images with higher magnification (x14), compared to the initial (x1) are shown. Green fluorescent dots in PS-treated cells represent fluorescent tagged PS beads. Scale bar is 150 μm. (B) Quantified data of (A). Mean and S.E. are shown (Tuj1; N = 2, Olig2; N = 3). (C) Cytotoxicity of 1 μm PS-MPs during differentiation (N = 3). Statistical analysis was done using one-way ANOVA and Bonferroni correction for pair-wise comparison to Cont, no beads control (**$p < 0.01$, *$p < 0.05$).

significantly decrease neurogenesis, with a reduction observed only when applied to differentiated cells for 5 days. Although smaller particles can penetrate cells and tissues more easily, resulting in higher toxicity, the observed cytotoxicity is contingent upon cell types and polymer types [28]. Previous studies have shown that 50 nm PS-NPs, but not 2 μm PS-MPs, exhibited cytotoxicity on C17.2 neuronal progenitor cells from the neonatal mouse cerebellum [29]. Additionally, 0.1 μm PS-NPs reduced the number of neural precursor cells and neuronal cells in a brain organoid model [30]. Both 50 nm and 500 nm PS-NPs decreased total cell numbers and neurite length in cultured hippocampal NSCs [31]. In the case of SVZ NSCs, 1 μm PS-MPs demonstrated greater cytotoxicity compared to 0.1 μm PS-NPs, while 2 μm PS-MPs exhibited the least effects.

Interestingly, only 0.1 μm NPs appeared to be endocytosed by NSCs, as demonstrated by their co-localization with Lysotracker, a marker for acidic intracellular vesicles. Conversely, 1 μm and 2 μm MP did not exhibit internalization by proliferating, differentiating,

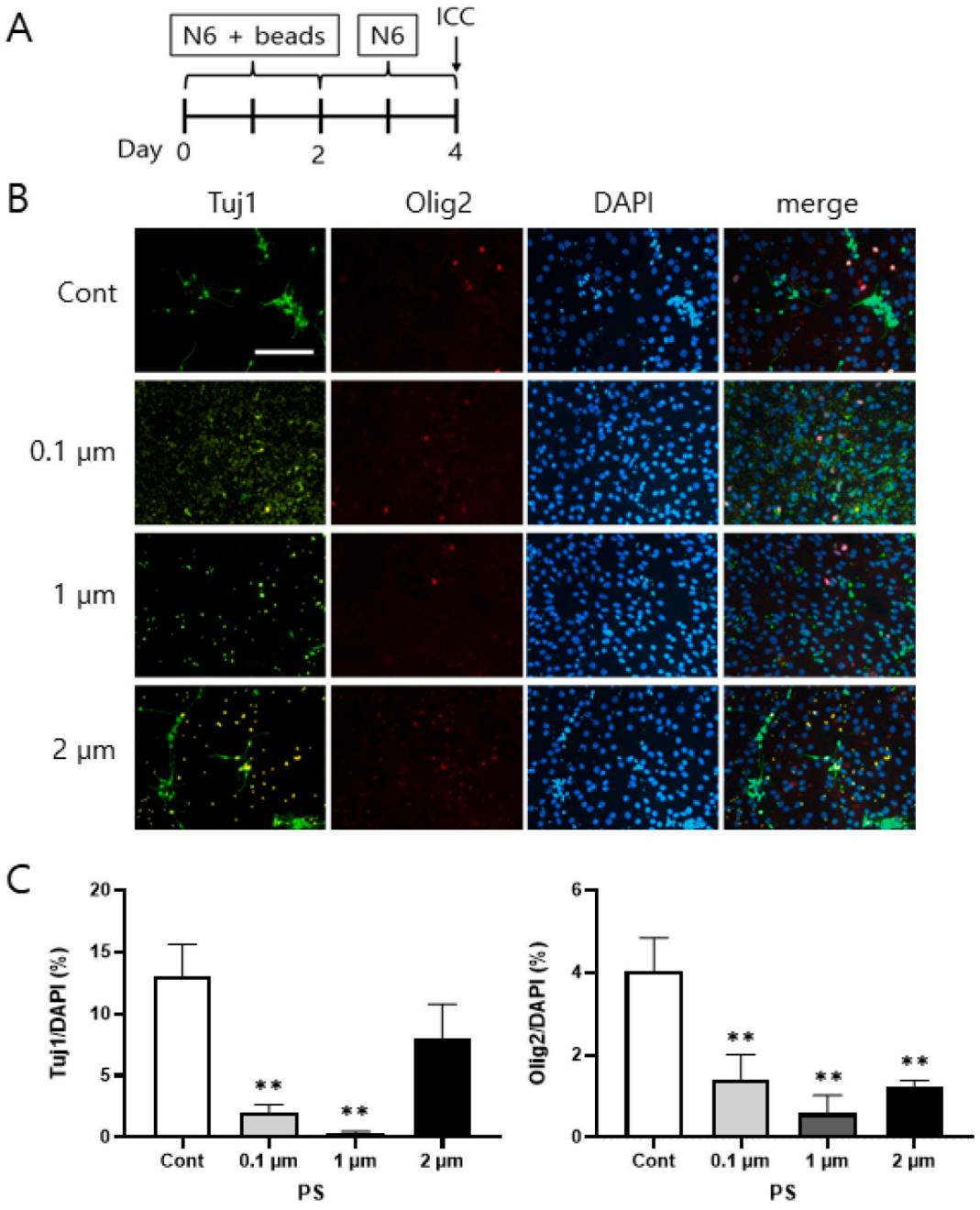

Fig. 6. (A) Experimental scheme. (B and C) Reduced the number of Tuj1-positive cells and Olig2-positive cells by transient exposure of SVZ NSCs to PS-MPs and –NPs (0.1 μm, 1 μm, and 2 μm sizes) at 10 μg/ml. (B) Green fluorescent dots in PS-treated cells represent fluorescent tagged PS beads. Scale bar is 25 μm. (C) Mean and S.E. are shown (N = 3). Statistical analysis was done using one-way ANOVA and Bonferroni correction for pair-wise comparison to no beads control (**$p < 0.01$).

or differentiated NSCs. This observation aligns with previous findings indicating that 2 μm PS-MPs did not penetrate the cellular membrane [20], and 0.1 μm PS-NPs, but not 1 μm PS-MPs, are found within human hepatic cells (HL7702) [32]. Upon internalization, PS-MPs may induce cytotoxicity through various mechanisms, including oxidative stress [33], ER stress [34], and damage to mitochondrial and nuclear DNA [32]. Specifically, 1 μm PS-MPs appear to compromise plasma membrane integrity without internalization, as evidenced by the increased LDH cytotoxicity observed in Fig. 5. Previous studies have shown that large PS-MPs cause plasma membrane deformation due to electrostatic interactions between amine-modified PS-MPs and negative charges in the plasma membrane [35]. Additionally, 500 nm PS-NPs have been reported to reduce cell membrane integrity in HUVECs (human umbilical vein endothelial cells) [36]. Thus, the compromised plasma membrane integrity introduced by 1 μm MP likely contributes to the diminished

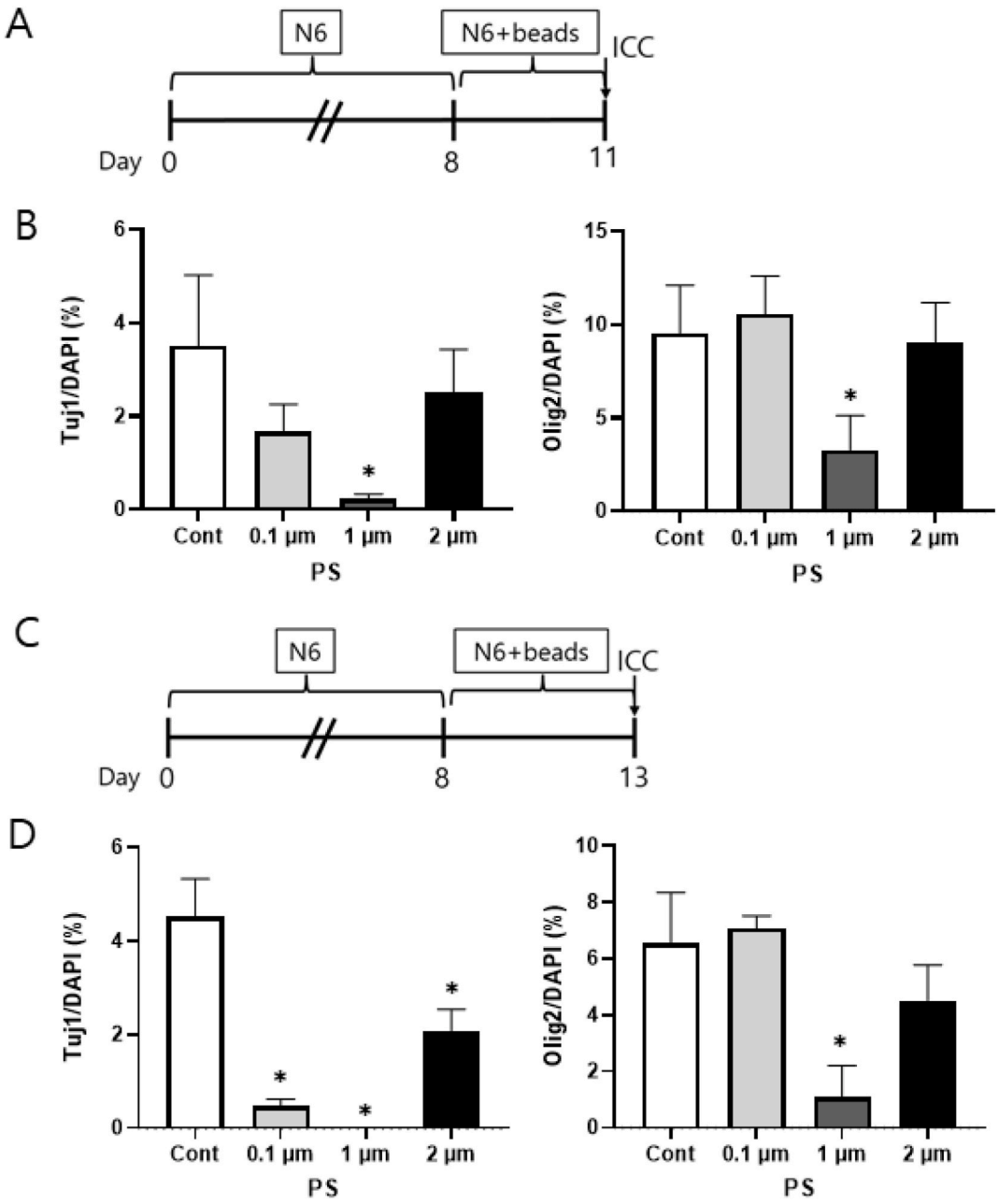

Fig. 7. (A) Experimental scheme for (B). (B) The numbers of Tuj1-positive neurons and Olig2-positive oligodendrocytes decreased in NSCs exposed to 1 μm PS-MPs. (C) Experimental scheme for (D). (D) PS-MPs and –NPs decreased the number of Tuj1-positive neurons and 1 μm PS-MPs decreased Olig2-positive oligodendrocytes. (B) and (D) Mean and S.E. are shown (N = 3 for B, N = 2 for D). Statistical analysis was done using one-way ANOVA and Bonferroni correction for pair-wise comparison to no beads control (*$p < 0.05$).

differentiation of NSCs and the neurotoxic effects observed in differentiated neurons and glial cells (Figs. 5–7). Conversely, the negligible increase in LDH cytotoxicity observed in cells treated with 2 μm MP aligns with the minimal effects of these particles on mSVZ differentiation and the neurotoxicity of differentiated neurons.

Regarding the surface charge of MPs and NPs, our results indicated that only positively charged amine-modified particles decreased the cell viability, whereas negatively charged carboxylate- or sulfate-modified particles did not. Similar findings have been reported, where positively charged PS-MPs and NPs exhibited higher toxicity compared to neutral or negatively charged counterparts in human intestinal epithelial cells (Caco-2) [37] and human alveolar cells [38]. The observed impact of surface charge on the toxicity of PS-MPs may be attributed to electrostatic interactions between positively charged MPs and negatively charged phospholipid in the plasma membrane [35]. Additionally, polysialylated-neural cell adhesion molecule (PSA-NCAM) is expressed in the SVZ [39], and polysialic

acid carries a highly negative charge, potentially enhancing the attraction of positively charged PS-MPs.

In this research, we utilized concentrations of 5 and 10 μg/mL for most of our experiments. While these concentrations may appear high compared to physiological levels, recent studies have estimated that humans may ingest 0.1∼5g of microplastics weekly [5]. Additionally, one study found approximately 300 μg/mL of 23 nm PS-NPs in the brains of mice when administered daily at a dose of 14.6 ng/kg for three days [40]. Another study reported that oral gavage of 2 μm PS-MPs to mice increased blood-brain barrier permeability and facilitated penetration of the particles into brain tissue [41]. Despite these findings, we acknowledge that concentrations of 5 and 10 μg/mL may be unrealistically high for human brain tissue. Therefore, accurate measurements are needed to determine the environmental concentrations of PS-MPs and NPs in animal brain tissues.

With the rapid accumulation of research reports on the biological effects of MPs and NPs, their impact on nervous system is still in its infancy. In the current study, we investigated the cytotoxic and neurotoxic effects of PS-MPs and –NPs on the NSCs of the SVZ. Our results suggest that NPs and MPs can have negative impacts on the neurogenic region of the brain by reducing cell viability, neuronal and glial differentiation, and possibly damaging neurons themselves. Although further investigation is needed to elucidate the detailed cellular mechanisms underlying this cytotoxicity, these findings provide clear evidence of the detrimental effects of MPs and NPs on the nervous system.

Funding

This research was supported by Research Program at the Korea Science Academy of KAIST with funding from the Korean Government (Ministry of Science and ICT) and by Basic Science Research Program through the National Research Foundation of Korea (NRF) funded by the Ministry of Science and ICT (NRF-2015R1C1A1A02037078).

Ethics statement

The euthanizing process of animal pups was performed in accordance with the protocol approved by Inje University Animal Care and Use Committee (approval ID number: Inje 2020-006) with minimal animal pain and suffering.

Data availability statement

All data generated in this study has not been deposited into any publicly available repository.
Data included in article/supp. material/referenced in article.

CRediT authorship contribution statement

Ki-Youb Park: Writing – review & editing, Writing – original draft, Project administration, Methodology, Investigation, Funding acquisition, Formal analysis, Data curation, Conceptualization. **Man Su Kim:** Resources, Funding acquisition. **Nuri Oh:** Investigation.

Declaration of competing interest

The authors declare that they have no known competing financial interests or personal relationships that could have appeared to influence the work reported in this paper.

Acknowledgments

We would like to give special thanks to Moonjung Kim, Haerin Seo, and Sohyun Jeon for their preliminary results that made this study possible.

References

[1] A.D. Vethaak, J. Legler, Microplastics and human health, Science. 371 (6530) (2021 Feb 12) 672–674, https://doi.org/10.1126/science.abe5041.
[2] S. Xu, J. Ma, R. Ji, K. Pan, A.J. Miao, Microplastics in aquatic environments: occurrence, accumulation, and biological effects, Sci. Total Environ. 703 (2020 Feb 10) 134699, https://doi.org/10.1016/j.scitotenv.2019.134699. Epub 2019 Nov 5. PMID: 31726297.
[3] Z. Maghsodian, A.M. Sanati, S. Tahmasebi, M.H. Shahriari, B. Ramavandi, Study of microplastics pollution in sediments and organisms in mangrove forests: a review, Environ. Res. 208 (2022 May 15) 112725, https://doi.org/10.1016/j.envres.2022.112725. Epub 2022 Jan 19. PMID: 35063433.
[4] L.F. Amato-Lourenço, R. Carvalho-Oliveira, G.R. Júnior, L. Dos Santos Galvão, R.A. Ando, T. Mauad, Presence of airborne microplastics in human lung tissue, J. Hazard Mater. 416 (2021 Aug 15) 126124, https://doi.org/10.1016/j.jhazmat.2021.126124. Epub 2021 May 24. PMID: 34492918.
[5] K. Senathirajah, S. Attwood, G. Bhagwat, M. Carbery, S. Wilson, T. Palanisami, Estimation of the mass of microplastics ingested - a pivotal first step towards human health risk assessment, J. Hazard Mater. 404 (Pt B) (2021 Feb 15) 124004, https://doi.org/10.1016/j.jhazmat.2020.124004. Epub 2020 Oct 6. PMID: 33130380.
[6] Z. Huang, Y. Weng, Q. Shen, Y. Zhao, Y. Jin, Microplastic: a potential threat to human and animal health by interfering with the intestinal barrier function and changing the intestinal microenvironment, Sci. Total Environ. 785 (2021 Sep 1) 147365, https://doi.org/10.1016/j.scitotenv.2021.147365. Epub 2021 Apr 27. PMID: 33933760.
[7] X. Zhu, C. Wang, X. Duan, B. Liang, E. Genbo Xu, Z. Huang, Micro- and nanoplastics: a new cardiovascular risk factor? Environ. Int. 171 (2023 Jan) 107662 https://doi.org/10.1016/j.envint.2022.107662. Epub 2022 Nov 26. PMID: 36473237.

[8] R. Kumar, C. Manna, S. Padha, A. Verma, P. Sharma, A. Dhar, A. Ghosh, P. Bhattacharya, Micro(nano)plastics pollution and human health: how plastics can induce carcinogenesis to humans? Chemosphere 298 (2022 Jul) 134267 https://doi.org/10.1016/j.chemosphere.2022.134267. Epub 2022 Mar 14. PMID: 35301996.

[9] L.F. Amato-Lourenço, L. Dos Santos Galvão, L.A. de Weger, P.S. Hiemstra, M.G. Vijver, T. Mauad, An emerging class of air pollutants: potential effects of microplastics to respiratory human health? Sci. Total Environ. 749 (2020 Dec 20) 141676 https://doi.org/10.1016/j.scitotenv.2020.141676. Epub 2020 Aug 13. PMID: 32827829; PMCID: PMC7424328.

[10] K. Kik, B. Bukowska, P. Sicińska, Polystyrene nanoparticles: sources, occurrence in the environment, distribution in tissues, accumulation and toxicity to various organisms, Environ. Pollut. 262 (2020 Jul) 114297, https://doi.org/10.1016/j.envpol.2020.114297. Epub 2020 Mar 2. PMID: 32155552.

[11] S.A. Siddiqui, S. Singh, N.A. Bahmid, D.J.H. Shyu, R. Domínguez, J.M. Lorenzo, J.A.M. Pereira, J.S. Câmara, Polystyrene microplastic particles in the food chain: characteristics and toxicity - a review, Sci. Total Environ. 892 (2023 Sep 20) 164531, https://doi.org/10.1016/j.scitotenv.2023.164531. Epub 2023 May 31. PMID: 37268142.

[12] Y. Zhao, Z. Bao, Z. Wan, Z. Fu, Y. Jin, Polystyrene microplastic exposure disturbs hepatic glycolipid metabolism at the physiological, biochemical, and transcriptomic levels in adult zebrafish, Sci. Total Environ. 710 (2020 Mar 25) 136279, https://doi.org/10.1016/j.scitotenv.2019.136279. Epub 2019 Dec 27. PMID: 31918190.

[13] L. Yin, H. Liu, H. Cui, B. Chen, L. Li, F. Wu, Impacts of polystyrene microplastics on the behavior and metabolism in a marine demersal teleost, black rockfish (Sebastes schlegelii), J. Hazard Mater. 380 (2019 Dec 15) 120861, https://doi.org/10.1016/j.jhazmat.2019.120861. Epub 2019 Jul 2. PMID: 31288171.

[14] Z. Li, S. Zhu, Q. Liu, J. Wei, Y. Jin, X. Wang, L. Zhang, Polystyrene microplastics cause cardiac fibrosis by activating Wnt/β-catenin signaling pathway and promoting cardiomyocyte apoptosis in rats, Environ. Pollut. 265 (Pt A) (2020 Oct) 115025, https://doi.org/10.1016/j.envpol.2020.115025. Epub 2020 Jun 18. PMID: 32806417.

[15] L. Lu, Z. Wan, T. Luo, Z. Fu, Y. Jin, Polystyrene microplastics induce gut microbiota dysbiosis and hepatic lipid metabolism disorder in mice, Sci. Total Environ. (631–632) (2018 Aug 1) 449–458, https://doi.org/10.1016/j.scitotenv.2018.03.051. Epub 2018 Mar 16. PMID: 29529433.

[16] J. Domenech, M. de Britto, A. Velázquez, S. Pastor, A. Hernández, R. Marcos, C. Cortés, Long-term effects of polystyrene nanoplastics in human intestinal caco-2 cells, Biomolecules 11 (10) (2021 Oct 1) 1442, https://doi.org/10.3390/biom11101442. PMID: 34680075; PMCID: PMC8533059.

[17] C.D. Dong, C.W. Chen, Y.C. Chen, H.H. Chen, J.S. Lee, C.H. Lin, Polystyrene microplastic particles: in vitro pulmonary toxicity assessment, J. Hazard Mater. 385 (2020 Mar 5) 121575, https://doi.org/10.1016/j.jhazmat.2019.121575. Epub 2019 Nov 3. PMID: 31727530.

[18] S. Wang, Q. Han, Z. Wei, Y. Wang, J. Xie, M. Chen, Polystyrene microplastics affect learning and memory in mice by inducing oxidative stress and decreasing the level of acetylcholine, Food Chem. Toxicol. 162 (2022 Apr) 112904, https://doi.org/10.1016/j.fct.2022.112904. Epub 2022 Mar 4. PMID: 35257813.

[19] S. Shan, Y. Zhang, H. Zhao, T. Zeng, X. Zhao, Polystyrene nanoplastics penetrate across the blood-brain barrier and induce activation of microglia in the brain of mice, Chemosphere 298 (2022 Jul) 134261, https://doi.org/10.1016/j.chemosphere.2022.134261. Epub 2022 Mar 14. PMID: 35302003.

[20] Y.H. So, H.S. Shin, S.H. Lee, H.J. Moon, H.J. Jang, E.H. Lee, E.M. Jung, Maternal exposure to polystyrene microplastics impairs social behavior in mouse offspring with a potential neurotoxicity, Neurotoxicology 99 (2023 Nov 1) 206–216, https://doi.org/10.1016/j.neuro.2023.10.013. Epub ahead of print. PMID: 37918694.

[21] T. Hua, S. Kiran, Y. Li, Q.A. Sang, Microplastics exposure affects neural development of human pluripotent stem cell-derived cortical spheroids, J. Hazard Mater. 435 (2022 Aug 5) 128884, https://doi.org/10.1016/j.jhazmat.2022.128884. Epub 2022 Apr 11. PMID: 35483261.

[22] X. Chen, L. Xu, Q. Chen, S. Su, J. Zhuang, D. Qiao, Polystyrene micro- and nanoparticles exposure induced anxiety-like behaviors, gut microbiota dysbiosis and metabolism disorder in adult mice, Ecotoxicol. Environ. Saf. 259 (2023 Jul 1) 115000, https://doi.org/10.1016/j.ecoenv.2023.115000. Epub 2023 May 19. PMID: 37210994.

[23] O. Baş, H. İlhan, H. Hancı, H. Çelikkan, D. Ekinci, M. Değermenci, B.O. Karapınar, A.A. Warille, S. Çankaya, S. Özkasapoğlu, To what extent are orally ingested nanoplastics toxic to the hippocampus in young adult rats? J. Chem. Neuroanat. 132 (2023 Oct) 102314 https://doi.org/10.1016/j.jchemneu.2023.102314. Epub 2023 Jul 19. PMID: 37473873.

[24] K. Obernier, A. Alvarez-Buylla, Neural stem cells: origin, heterogeneity and regulation in the adult mammalian brain, Development 146 (4) (2019 Feb 18) dev156059, https://doi.org/10.1242/dev.156059. PMID: 30777863; PMCID: PMC6398449.

[25] D.A. Lim, Y.C. Huang, T. Swigut, A.L. Mirick, J.M. Garcia-Verdugo, J. Wysocka, P. Ernst, A. Alvarez-Buylla, Chromatin remodelling factor Mll1 is essential for neurogenesis from postnatal neural stem cells, Nature 458 (7237) (2009 Mar 26) 529–533, https://doi.org/10.1038/nature07726. Epub 2009 Feb 11. PMID: 19212323; PMCID: PMC3800116.

[26] K.Y. Park, S. Kim, M.S. Kim, Effects of taxol on neuronal differentiation of postnatal neural stem cells cultured from mouse subventricular zone, Differentiation 119 (2021 May-Jun) 1–9, https://doi.org/10.1016/j.diff.2021.03.001. Epub 2021 Apr 8. PMID: 33848959.

[27] K.Y. Park, M.S. Kim, Inhibition of proliferation and neurogenesis of mouse subventricular zone neural stem cells by a mitochondrial inhibitor rotenone, J. Life Sci. 28 (12) (2018) 1397–1405, https://doi.org/10.5352/JLS.2018.28.12.1397.

[28] A. Banerjee, W.L. Shelver, Micro- and nanoplastic induced cellular toxicity in mammals: a review, Sci. Total Environ. 755 (Pt 2) (2021 Feb 10) 142518, https://doi.org/10.1016/j.scitotenv.2020.142518. Epub 2020 Sep 25. PMID: 33065507.

[29] S. Yang, S. Lee, Y. Lee, J.H. Cho, S.H. Kim, E.S. Ha, Y.S. Jung, H.Y. Chung, M.S. Kim, H.S. Kim, S.C. Chang, K.J. Min, J. Lee, Cationic nanoplastic causes mitochondrial dysfunction in neural progenitor cells and impairs hippocampal neurogenesis, Free Radic. Biol. Med. 208 (2023 Nov 1) 194–210, https://doi.org/10.1016/j.freeradbiomed.2023.08.010. Epub 2023 Aug 6. PMID: 37553025.

[30] S. Chen, Y. Chen, Y. Gao, B. Han, T. Wang, H. Dong, L. Chen, Toxic effects and mechanisms of nanoplastics on embryonic brain development using brain organoids model, Sci. Total Environ. 904 (2023 Dec 15) 166913, https://doi.org/10.1016/j.scitotenv.2023.166913. Epub 2023 Sep 7. PMID: 37689192.

[31] B. Jeong, J.Y. Baek, J. Koo, S. Park, Y.K. Ryu, K.S. Kim, S. Zhang, C. Chung, R. Dogan, H.S. Choi, D. Um, T.K. Kim, W.S. Lee, J. Jeong, W.H. Shin, J.R. Lee, N. S. Kim, D.Y. Lee, Maternal exposure to polystyrene nanoplastics causes brain abnormalities in progeny, J. Hazard Mater. 426 (2022 Mar 15) 127815, https://doi.org/10.1016/j.jhazmat.2021.127815. Epub 2021 Nov 18. PMID: 34823950.

[32] R. Shen, K. Yang, X. Cheng, C. Guo, X. Xing, H. Sun, D. Liu, X. Liu, D. Wang, Accumulation of polystyrene microplastics induces liver fibrosis by activating cGAS/STING pathway, Environ. Pollut. 300 (2022 May 1) 118986, https://doi.org/10.1016/j.envpol.2022.118986. Epub 2022 Feb 12. PMID: 35167931.

[33] Y.C. Chen, K.F. Chen, K.A. Lin, J.K. Chen, X.Y. Jiang, C.H. Lin, The nephrotoxic potential of polystyrene microplastics at realistic environmental concentrations, J. Hazard Mater. 427 (2022 Apr 5) 127871, https://doi.org/10.1016/j.jhazmat.2021.127871. Epub 2021 Nov 25. PMID: 34862106.

[34] S.L. Lim, C.T. Ng, L. Zou, Y. Lu, J. Chen, B.H. Bay, H.M. Shen, C.N. Ong, Targeted metabolomics reveals differential biological effects of nanoplastics and nanoZnO in human lung cells, Nanotoxicology 13 (8) (2019 Oct) 1117–1132, https://doi.org/10.1080/17435390.2019.1640913. Epub 2019 Jul 24. PMID: 31272252.

[35] S. Li, N. Malmstadt, Deformation and poration of lipid bilayer membranes by cationic nanoparticles, Soft Matter 9 (20) (2013) 4969–4976.

[36] Y.Y. Lu, H. Li, H. Ren, X. Zhang, F. Huang, D. Zhang, Q. Huang, X. Zhang, Size-dependent effects of polystyrene nanoplastics on autophagy response in human umbilical vein endothelial cells, J. Hazard Mater. 421 (2022 Jan 5) 126770, https://doi.org/10.1016/j.jhazmat.2021.126770. Epub 2021 Jul 31. PMID: 34358975.

[37] D. Xu, Y. Ma, X. Han, Y. Chen, Systematic toxicity evaluation of polystyrene nanoplastics on mice and molecular mechanism investigation about their internalization into Caco-2 cells, J. Hazard Mater. 417 (2021 Sep 5) 126092, https://doi.org/10.1016/j.jhazmat.2021.126092. Epub 2021 May 13. PMID: 34015712.

[38] A. Roshanzadeh, S. Park, S.E. Ganjbakhsh, J. Park, D.H. Lee, S. Lee, E.S. Kim, Surface charge-dependent cytotoxicity of plastic nanoparticles in alveolar cells under cyclic stretches, Nano Lett. 20 (10) (2020 Oct 14) 7168–7176, https://doi.org/10.1021/acs.nanolett.0c02463. Epub 2020 Sep 10. PMID: 32876460.

[39] L. Bonfanti, D.T. Theodosis, Expression of polysialylated neural cell adhesion molecule by proliferating cells in the subependymal layer of the adult rat, in its rostral extension and in the olfactory bulb, Neuroscience 62 (1) (1994 Sep) 291–305, https://doi.org/10.1016/0306-4522(94)90333-6. PMID: 7816207.

[40] F.N. Estrela, A.T.B. Guimarães, A.P.D.C. Araújo, F.G. Silva, T.M.D. Luz, A.M. Silva, P.S. Pereira, G. Malafaia, Toxicity of polystyrene nanoplastics and zinc oxide to mice, Chemosphere 271 (2021 May) 129476, https://doi.org/10.1016/j.chemosphere.2020.129476. Epub 2020 Dec 30. PMID: 33434826.

[41] C.W. Lee, L.F. Hsu, I.L. Wu, Y.L. Wang, W.C. Chen, Y.J. Liu, L.T. Yang, C.L. Tan, Y.H. Luo, C.C. Wang, H.W. Chiu, T.C. Yang, Y.Y. Lin, H.A. Chang, Y.C. Chiang, C. H. Chen, M.H. Lee, K.T. Peng, C.C. Huang, Exposure to polystyrene microplastics impairs hippocampus-dependent learning and memory in mice, J. Hazard Mater. 430 (2022 May 15) 128431, https://doi.org/10.1016/j.jhazmat.2022.128431. Epub 2022 Feb 4. Erratum in: J Hazard Mater. 2023 Jul 5;453:131398. PMID: 35150991.